QUARTERLY JOURNAL
OF THE
ROYAL METEOROLOGICAL SOCIETY

Vol. 110 JULY 1984 No. 465

Quart. J. R. Met. Soc. (1984), **110**, pp. 573–590 551.465

Eddy–mean-flow interaction in a barotropic ocean model

By J. C. MARSHALL
Atmospheric Physics Group, Imperial College, London

(Received July 20 1983; revised 31 January 1984. Communicated by Dr F. W. Taylor)

SUMMARY

The role of eddies in the maintenance of idealized, antisymmetrically forced double gyres is studied using a barotropic ocean circulation model. A diagnosis in terms of q, the quasi-conserved absolute vorticity, enables an understanding of the effect of the eddies on the time-mean flow. The unstable model Gulf Stream, partitioning counter-rotating gyres, is the confluence region where q contours from widely differing latitudes become concentrated, interwoven and irreversibly deformed. Here there is a strong enstrophy cascade, large eddy fluxes and eddy flux divergences, and significant driving of mean flow by the eddies. This barotropic instability of the internal jet results in a lateral transfer of vorticity sufficient to balance the net forcing of the subtropical gyre by the wind-stress curl. The separation of the eddy flux into non-divergent 'advection' and divergent 'conversion' contributions, using the eddy enstrophy equation as a dynamical reference, makes transparent the sense of the local eddy q flux and its systematic effect on time-mean flow.

1. INTRODUCTION

The high resolution models designed to resolve the oceanic geostrophic eddy field have given new insights into its role and interaction with the large-scale gyres. Classical wind-driven circulation theory, for example Munk (1950), relegated eddy variability to a means of providing a pathway to small-scale dissipation confined to western boundary currents. In contrast, the eddy-resolving models emphasize the importance of the eddy field as a transferring agent *redistributing* properties within and between gyres, rather than as a mechanism of overall vorticity loss. Harrison (1981), for example, has highlighted the possible role of the meandering Gulf Stream in the redistribution of vorticity offsctting the imbalance in the wind-stress curl vorticity source, cyclonic to the north of the stream and anticyclonic to the south. One is reminded of the poleward transfer of heat by the atmospheric geostrophic eddy field, the mid-latitude synoptic systems, to offset the net warming of equatorial regions and the net cooling of polar regions. The oceanic eddy field could thus play an analogous role in the large-scale ocean circulation to that of synoptic systems in the large-scale circulation of the atmosphere.

Although these analogies are helpful in thinking about the eddy field in the context of the gyre-scale circulation, the intuition gained from meteorological experience can also be misleading. The ocean, unlike the atmosphere, is zonally blocked by coasts which can support a zonal pressure gradient, leading directly to a geostrophically balanced meridional velocity. The success of the interior Sverdrup balance (Sverdrup 1947) in explaining the position, sense of rotation and mass transport of the major ocean gyres (see, for example, Welander 1959) shows that the first-order circulation can be understood without the need to invoke eddy transfer. In the zonally periodic atmosphere, however, it is necessary to invoke eddy transfer from the outset to support the zonal mean surface

winds, which only then help drive the mean meridional circulation frictionally from the ground (Jeffreys 1926; Eady 1953; Green 1970).

The prevalence of Sverdrup dynamics in the ocean implies that the interior meridional drift must return in intense western boundary currents. It is the instability of these boundary currents and their seaward extensions that supply eddies to populate the basin. Unlike the troposphere, which is dynamically unstable everywhere in the zonal time mean, conditions for instability in the ocean are most easily satisfied in jet regions. Although the atmospheric long-wave pattern organizes weather systems into storm tracks with beginnings and ends, zonal variations in the ocean due to coasts and boundary currents are more severe, regions of eddy generation more localized, and the regions of eddy decay more extensive.

Much of the development of our understanding of the transfer properties and eddy–mean-flow interaction of atmospheric weather systems has had at its foundation insights gained from the instability analyses of zonal flows, which are simply not relevant to the strong curved oceanic flows. Holland and Rhines (1980) demonstrate the added complexity introduced by strong curved flows in the upper layer of a two-layer quasi-geostrophic ocean model, where the potential vorticity contours run significantly north–south. Our meteorological experience only holds good in the lower layer, where mean flow is sufficiently weak for the potential vorticity contours to run east–west.

Here a numerical experiment with an eddy-resolving barotropic model is described, which we hope helps to unravel some of these complexities. Although the model is barotropic, it provides the most appropriate and useful reference for the layered quasi-geostrophic ocean models. It is particularly relevant to the upper layer of Holland's (1978) two-layer model. The work is an extension of the single, steady gyre barotropic calculations begun by Bryan (1963) and continued notably by Veronis (1966) and Blandford (1971), to include a dynamically active internal jet partitioning counter-rotating gyres. The barotropic instability of the jet transfers all the vorticity required to maintain the equilibrium of the model subtropical gyre. The model formulation and diagnostic approach is described in section 2. In section 3 the maintenance of the time-mean gyres by wind and eddy transfer is studied in detail. The spatial distribution of eddy fluxes and their relation to mean gradients is rationalized with reference to the eddy enstrophy equation, and suggests the parametric representation of eddy–mean-flow interaction discussed in section 4.

2. Barotropic ocean model

Our ocean model is a layer of homogeneous fluid confined to a rectangular, flat bottomed basin and governed by the barotropic vorticity equation. It is driven by an imposed wind-stress curl and frictionally retarded. The barotropic vorticity equation has been the basis of much of classical wind-driven ocean circulation theory and is derived in, for example, Bryan (1963) and Veronis (1966). Conveniently non-dimensionalized, it may be written

$$R^{-1}\partial q/\partial t + J(\psi, q) = F - D, \tag{1}$$

expressing the conservation of q but for forcing and dissipation, where

$J(\psi, q) = (\partial\psi/\partial x)(\partial q/\partial y) - (\partial\psi/\partial y)(\partial q/\partial x)$ is the Jacobian
ψ is the streamfunction
$q = R\zeta + y$ is the absolute vorticity
$\zeta = \nabla^2\psi$ is the relative vorticity

$R = \pi\tau(\rho H\beta^2 L^3)^{-1}$ is a Rossby number for the vorticity equation measuring the magnitude of the relative vorticity gradient relative to the planetary vorticity gradient

$F = -\partial\tau/\partial y$ is the wind-stress curl forcing

where x is east, y is north, $\tau = \tau(y)$ is the zonal wind-stress; ρ, the density; H, the layer depth; β, the planetary vorticity gradient; L, the width of the basin; and

$D = \varepsilon\zeta + A_4\nabla^4\zeta$ is the frictional dissipation

where ε and A_4 are bottom and lateral (biharmonic) frictions respectively.

In Eq. (1) the velocity has been non-dimensionalized with the Sverdrup velocity scale, $\pi\tau/\rho\beta HL$, and the distance and time by L and $(\beta L)^{-1}$ respectively.

(*a*) *Sub-grid-scale parametrizations and boundary conditions*

In order that the model can become dynamically unstable it must be weakly dissipative so that advection can dominate even in boundary currents. This allows physically resolved motions to transport q rather than this be represented by *ad hoc* parametrizations. Accordingly, a scale-selective lateral friction is introduced, $A_4\nabla^4\zeta$, which remains small in the vorticity equation (1) at dynamically interesting scales. Unlike the lateral friction of Munk (1950), the term is not imagined to represent the lateral transfer of momentum to a coast, but rather to dissipate the enstrophy that inevitably builds up at small (grid) scales in highly turbulent flows. Along with this reinterpretation of the lateral friction it seems appropriate to make the boundaries slippery so as to minimize the influence of frictional boundary layers in the dynamics of the gyre. Rather than impose an arbitrary condition on the boundary vorticity it is preferred to integrate Eq. (1) *at* the boundary, allowing the boundary vorticity to evolve in time.

The enstrophy-destroying fourth-order term requires two extra boundary conditions at each lateral wall, in addition to that of no normal flow,

$$\psi = \text{constant}. \tag{2a}$$

The following conditions are applied on vorticity gradient:

$$\partial\zeta/\partial n = \partial^3\zeta/\partial n^3 = 0, \tag{2b}$$

where n is the normal to the boundary. Condition (2b) ensures that the inclusion of the biharmonic friction does not itself result in any net dissipation of vorticity, because

$$\int_{\text{over domain}} \nabla^4\zeta \, dx\, dy = \oint_{\text{around boundary}} (\partial^3\zeta/\partial n^3)\, dl = 0.$$

Again this should be contrasted with the function of the lateral friction in classical wind-driven ocean circulation theory with the no-slip boundary condition, such as Munk (1950). There the net input of vorticity over each wind-driven gyre is dissipated in the lateral frictional boundary layer at the western boundary within each gyre.

The boundary integration of (1) and the boundary conditions (2) are unconventional, but are chosen because they minimize the importance of frictional boundary layers and maximize the role of eddy transfer in the maintenance of the time-mean gyres. The conventional 'free-slip' condition, $\zeta = 0$, places a much more rigid constraint on the geometry of the q contours because, for all time, $q = y$ at the east and west coast (see Marshall 1982). With the boundary integration, however, the q contours are not firmly attached to the coast at their reference latitude and so, in a sufficiently nonlinear boundary current, can be drawn almost parallel to the streamlines.

(*b*) *Method of solution*

A finite difference approximation of Eq. (1) with boundary conditions Eqs. (2), is solved on a square grid in both single and double gyre configurations (see Fig. 1):

(i) single anticyclonically forced subtropical gyre in domain

$$\left.\begin{aligned} 0 < x < 1 \\ -1 < y < 0 \end{aligned}\right\} \qquad (3a)$$

with $F = \sin(\pi y)$

(ii) antisymetrically forced double gyre in domain

$$\left.\begin{aligned} 0 < x < 1 \\ -1 < y < 1 \end{aligned}\right\} \qquad (3b)$$

with $F = \sin(\pi y)$

giving a northern cyclonically forced subpolar gyre, and a southern anticyclonically forced subtropical gyre.

Equation (1) is leap-frogged forward in time from an initial state of rest at interior and boundary points. At each time step a finite difference version of the Poisson equation

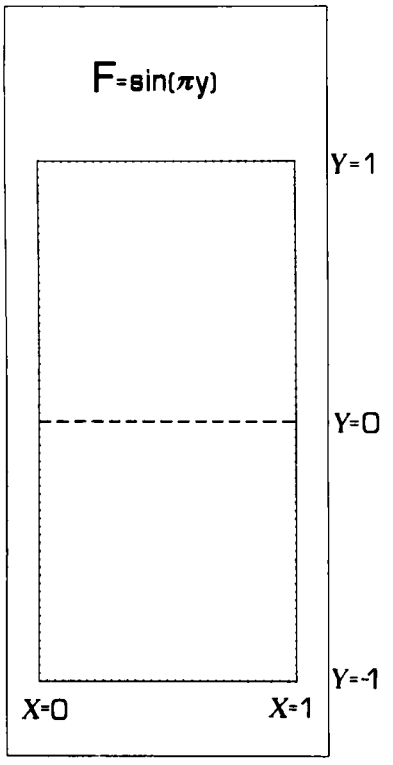

Figure 1. The geometry of the basin in relation to the wind-stress curl forcing, F. The dotted line is the northern boundary of the single gyre.

is inverted exactly to calculate ψ from q. The Jacobian is finite differenced using Arakawa's (1966) formulation. Corner points and walls of our closed basin must be treated separately, and with care, to ensure complete cancellation of the advection terms in the summation of the kinetic energy, enstrophy and vorticity integrals. The boundary conditions, Eqs. (2), permit the evaluation of the biharmonic term at the boundary and ensure that it cannot act as a net vorticity sink.

(c) *Diagnostics*

In order to examine the statistically steady state of the model, it is useful to separate mean and eddy processes by defining mean and eddy quantities

$$\psi = \overline{\psi} + \psi' \tag{4}$$

where overbar denotes a time average over many eddy life-times and prime, the deviation from the average. Eddy transfer is introduced by substituting (4) into (1) and time averaging to give

$$R^{-1}\partial\overline{q}/\partial t + J(\overline{\psi}, \overline{q}) + J(\overline{\psi', q'}) = \overline{F} - \overline{D}. \tag{5}$$

Equation (5) shows why there should be an interest in the geometry of the $\overline{q}$ contours, for these are the reference along which, but for eddies, forcing and dissipation, the mean flow moves. It is for this reason that there has recently been such interest in the large-scale ocean circulation viewed from the perspective of potential vorticity and its close conservation (see Rhines and Young 1982). In the present barotropic model it is the absolute vorticity which provides the constraint on mean flow and eddies.

In our study of the eddy–mean-flow interaction in the model, frequent reference will be made to the eddy enstrophy equation, since it provides a helpful dynamical basis to interpret the spatial pattern of eddy fluxes and their relation to the $\overline{q}$ geometry. It may be derived by first forming the prognostic equation for the eddies $\partial q'/\partial t$, Eqs. (1)–(5), multiplying by q' and time averaging to give, neglecting triple correlations:

$$\partial(\tfrac{1}{2}\overline{q'^2})/\partial t + \overline{\mathbf{v}} \cdot \nabla\tfrac{1}{2}\overline{q'^2} + \overline{\mathbf{v}'q'} \cdot \nabla\overline{q} = -\overline{D'q'} \tag{6}$$

where $\mathbf{v} = \mathbf{k} \wedge \nabla\psi$ is the horizontal geostrophic velocity. The eddy enstrophy equation relates the cross-gradient eddy q flux to the advection of eddy enstrophy by the mean flow, and its dissipation by the enstrophy cascade.

In the atmosphere, the zonal-averaged eddy q flux tends to be directed down gradient because the irreversible deformation of the q contours in turbulent flow promotes an enstrophy cascade: the zonal, long-time average of Eq. (6) takes the form

$$\overline{v'q'}^{xt}(\partial\overline{q}/\partial y) = -\overline{D'q'}^{xt} < 0. \tag{7}$$

This is the rationale behind the adoption of a down-gradient parametrization of the zonal-average eddy q flux due to synoptic eddies in the atmosphere: the flux must be directed down gradient to offset the continual dissipation of enstrophy at the small scales.

Rhines (1979) points out that the zonal asymmetry of the ocean circulation, introduced by meridional walls and western boundary currents, results in strong curved flows in which the advection of $\overline{q'^2}$ is an important term in Eq. (6). In fact mean flow advection cannot be ignored in local enstrophy budgets in the atmosphere either (see Illari and Marshall 1983), particularly at the beginning and end of the atmospheric storm tracks. The ocean is even less zonally uniform than the atmosphere and so advection in Eq. (6) correspondingly more important. Holland and Rhines (1980), for example, in a

diagnosis of a two-layer quasi-geostrophic eddy-resolving model, contrast the relative importance of the $\bar{\mathbf{v}} \cdot \nabla \tfrac{1}{2}\overline{q'^2}$ in upper and lower layers. In the upper layer the strongly circulatory gyres advect $\overline{q'^2}$ and, in response, the q fluxes are directed both up and down gradient. Only in the lower layer, where mean flow is weak and advection of $\overline{q'^2}$ small, does the eddy q flux point systematically down the $\bar{q}$ gradient.

Marshall and Shutts (1981) use Eq. (6) as a dynamical basis from which to rationalize the sense of the eddy q flux, and are able to associate the flow advection term with *rotational, non-divergent* fluxes. They show that if mean flow $\bar{\psi}$ does not deviate far from the $\bar{q}$ contours, i.e. there is a functional relationship $\bar{\psi} = \bar{\psi}(\bar{q})$, then Eq. (6) separates naturally into two parts:

$$\bar{\mathbf{v}} \cdot \nabla \tfrac{1}{2}\overline{q'^2} + (\overline{\mathbf{v}'q'})_{\text{rot}} \cdot \nabla \bar{q} = 0 \tag{8a}$$

$$\partial(\tfrac{1}{2}\overline{q'^2})/\partial t + (\overline{\mathbf{v}'q'} - (\overline{\mathbf{v}'q'})_{\text{rot}}) \cdot \nabla \bar{q} = -\overline{D'q'} \tag{8b}$$

where $(\overline{\mathbf{v}'q'})_{\text{rot}} = \tfrac{1}{2}\mathbf{k} \wedge \nabla\{(d\bar{\psi}/d\bar{q})\overline{q'^2}\}$ with $\mathbf{k}$ a unit vector pointing vertically upwards. Thus the $(\overline{\mathbf{v}'q'})_{\text{rot}}$, which may be called an 'advection' flux, responds to flow advection of $\overline{q'^2}$ but cannot drive time-mean flow, Eq. (5), because it is non-divergent. The remaining flux, $\overline{\mathbf{v}'q'} - (\overline{\mathbf{v}'q'})_{\text{rot}}$, which may be called a 'conversion' flux, contains all the divergent flux and, in common with the zonal average flux of Eq. (7), is directed down gradient if there is an enstrophy cascade. This rationalization of the eddy flux into dynamically distinct contributions has proved useful in diagnosing the effect of synoptic-scale systems on time-mean flow in atmospheric blocking (see Illari and Marshall 1983; Shutts 1983).

In section 3, diagnostics of the statistically steady state of the model will be presented in the following framework. We will be interested in:

(i) The geometry of the $\bar{q}$ contours, the extent to which they are the reference for the mean gyres $\bar{\psi}$, and the relative importance of wind forcing $\bar{F}$, dissipation $\bar{D}$ and eddy flux divergence $J(\overline{\psi', q'})$, in driving $\bar{\psi}$ across the $\bar{q}$ contours, breaking the functional relationship $\bar{\psi}(\bar{q})$.
(ii) The rationalization of the sense of $\overline{\mathbf{v}'q'}$ with respect to the advection of $\overline{q'^2}$ and its dissipation by the enstrophy cascade, provided by Eq. (6) and its decomposition, Eqs. (8).
(iii) The mechanism of overall vorticity equilibrium.

3. Maintenance of time-mean gyres

In this section two numerical integrations are described. In the first, Eq. (1) is solved in the domain (3a), spinning up a single steady Veronis (1966) gyre. In the second, Eq. (1) is solved in the domain (3b) and the flow becomes time dependent reaching a statistically steady state in which counter-rotating gyres exchange properties. In both integrations the non-dimensional coefficients are the same: their fundamentally different character arises because the eastward flowing boundary current along the northern wall of the single gyre becomes an unstable internal jet in the double gyre.

The following non-dimensional measure of the non-linearity is chosen: $R = \tfrac{1}{2}\pi \times 10^{-3}$, corresponding to an ocean in which, dimensionally, $\tau = 10^{-1}\,\text{N m}^{-2}$, $\rho = 10^3\,\text{kg m}^{-3}$, $\beta = 2\times10^{-11}\,\text{m}^{-1}\,\text{s}^{-1}$, $H = 5\times10^2\,\text{m}$, $L = 10^6\,\text{m}$.

The equations are integrated with a time step of 0·1 on a 33×33 grid for the single gyre, and a 33×65 grid for the double gyre. The horizontal resolution is just sufficient to resolve the inertial boundary layer, of width $R^{1/2}$.

The coefficients A_4 and ε are chosen so as not to become locally important terms in Eq. (1) and, in particular, A_4 is reduced to the minimum required to maintain a reasonably continuous vorticity field: they are (non-dimensionally) $\varepsilon = 10^{-2}$ and $A_4 = 3\times10^{-8}$.

(*a*) *Steady single gyre*

Figure 2 shows the $\bar{\psi}$ and $\bar{q}$ of the single gyre integration after reaching a steady state. The flow is strongly nonlinear with a northern boundary current extending across

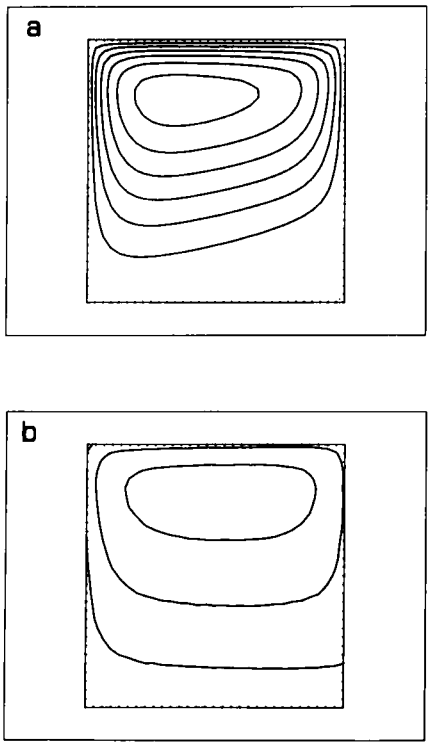

Figure 2. The single steady gyre. (a) $\bar{\psi}$: contour interval (C.I.) = 0·4; $\bar{\psi}_{max}$ = 2·6, showing that the gyre has spun up in excess of Sverdrup. (b) $\bar{q}$: C.I. = 0·2.

the entire length of the northern wall and returning to the interior from the east. The nonlinear boundary current thus penetrates the interior, destroying the linear Sverdrup balance in the northern half of the basin.

In the inertial recirculation, the important balance in Eq. (5) is $J(\bar{\psi}, \bar{q}) \simeq 0$ with $\bar{\psi} \simeq \bar{\psi}(\bar{q})$ and the $\bar{q}$ contours drawn almost parallel to the $\bar{\psi}$ contours. The flow is sufficiently nonlinear to resemble a Fofonoff (1954) free basin mode. It is interesting that although the 'parallel flow' criterion for instability ($d\bar{q}/dy$ changing sign) is satisfied, the flow is absolutely stable in the limit of the Fofonoff inviscid solution.

The amplitude of the solution is limited by the magnitude of the bottom friction coefficient ε. Integrating over the gyre,

$$\varepsilon \int \bar{\zeta}\, dx\, dy = \int \bar{F}\, dx\, dy. \tag{9}$$

We recall that the biharmonic friction cannot act as a vorticity sink because of the choice of boundary condition (2b).

The maximum streamfunction in the domain measures the transport of the gyre, quantifying the degree of spin-up. If the interior was in linear Sverdrup balance ($\bar{q} \simeq y$), the $\bar{\psi}_{max}$ would be unity: the $\bar{\psi}_{max}$ of the nonlinear gyre in Fig. 2 is 2·6. Pedlosky (1979) describes this spin-up in excess of Sverdrup as the 'singular perturbation' involved in ignoring lateral frictional boundary layers. Their absence in the single gyre has led to a circulation in which interior velocities must exceed Sverdrup in order to accomplish the necessary dissipation through bottom friction. In section 3(*b*) it will be shown that the neglect of frictional boundary layers in time-dependent double gyres need not lead to a spin-up vastly exceeding Sverdrup, because the circulation becomes dynamically unstable, allowing lateral vorticity exchange between gyres.

(*b*) *Time-dependent double gyres*

Figure 3 shows a sequence of instantaneous ψ and q maps taken after the flow has reached a statistically steady state. The boundary current flowing along the northern

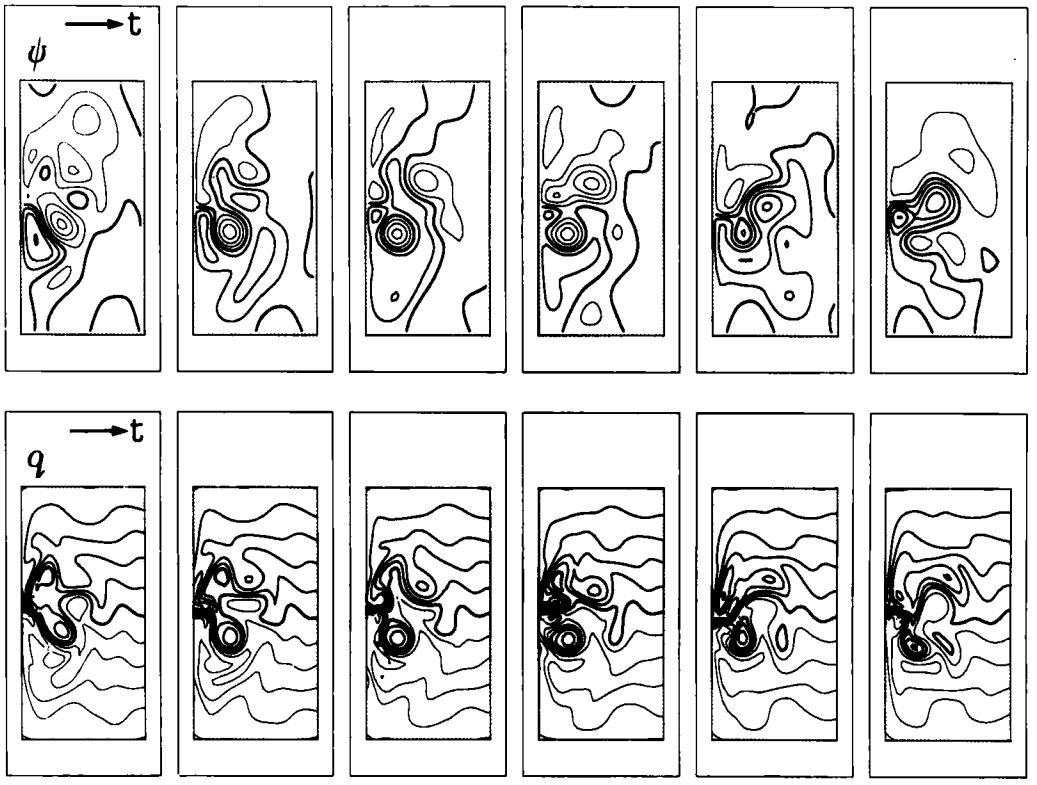

Figure 3. A series of instantaneous ψ(C.I. = 0·5) and q(C.I. = 0·2) fields from the double gyre integration at 16 time unit intervals. Thin lines represent negative contours, thick lines positive contours, and the very thick line the zero contour. The boundary current along the northern wall of Fig. 2 has become an unstable internal jet. There is irreversible deformation of the q contours in the jet, visible evidence of a strong enstrophy cascade. Away from the jet, to the north and south, westward propagating basin modes reversibly deform the q contours.

wall of the single steady gyre, Fig. 2, has become a barotropically unstable internal jet meandering along the zero wind-stress curl line, and occasionally forming cut-off rings. The diameter of each eddy scales as $(u/\beta)^{1/2}$ dimensionally, where u is a typical eddy speed.

(i) *Mean flow and the geometry of $\bar{q}$ contours.* The $\bar{\psi}$ and $\bar{q}$ calculated by averaging over many eddy life times, Fig. 4, shows two counter-rotating circulations corresponding to a northern subpolar and a southern subtropical gyre. Ideally the long-time mean should be antisymmetric about $y = 0$ but, due to the necessarily finite length of the averaging interval, this is not wholly achieved. It is the maintenance of these Eulerian mean gyres which is the main concern here. It is essential to consider the $\bar{\psi}$ in the context of the $\bar{q}$ contours. The $\bar{\psi}$ and $\bar{q}$ are superimposed in Fig. 4(c).

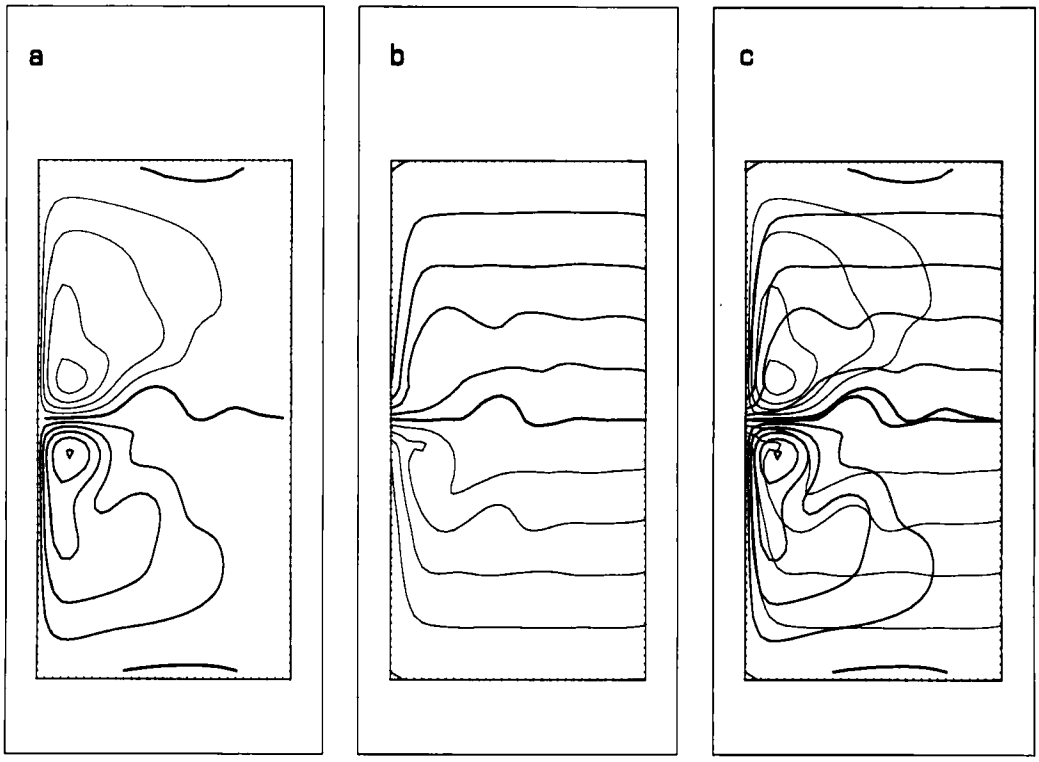

Figure 4. The mean fields from the double gyre integration calculated by averaging a sequence of 400 instantaneous fields at 4 time unit intervals. (a) $\bar{\psi}$: (C.I. = 0.3); (b) $\bar{q}$: (C.I. = 0.2); (c) $\bar{\psi}$ and $\bar{q}$ superimposed. In the regions of Sverdrup balance, $\bar{q} = y$ and the $\bar{\psi}$ is driven across $\bar{q}$ by the wind-stress curl, $\bar{F}$. The eddy term, $J(\psi', q')$, allows the $\bar{\psi}$ to recross the $\bar{q}$ in the unstable jet and return to the interior.

In the region of linear Sverdrup balance, $J(\bar{\psi}, \bar{q}) = \bar{F}$ with $\bar{q} = y$, the mean flow is weak and the $\bar{q}$ contours run west–east along latitude circles. Here the $\bar{\psi}$ are driven across the $\bar{q}$ by the wind-stress curl.

Mean flow from the Sverdrup interior turns northwards (in the subtropical gyre) in a strong western boundary current advecting its $\bar{q}$ contours with it. In this inflow region $J(\bar{\psi}, \bar{q}) \simeq 0$ with $\bar{q} = R\bar{\zeta} + y$, as in the early inertial boundary current theory of, for example, Charney (1955).

In the north-west of the subtropical gyre, the $\bar{q}$ contours are attached to the western lateral wall, and so here the flow must cross the $\bar{q}$ contours from lower to higher values in order to rejoin the Sverdrup interior. It is the eddy flux divergence of q which allows the $\bar{\psi}$ to cross the $\bar{q}$: the dominant balance is

$$J(\bar{\psi}, \bar{q}) + J(\overline{\psi', q'}) \simeq 0$$

with bottom and biharmonic friction an order of magnitude smaller than either term. This should be contrasted with classical, steady, wind-driven circulation theory (for example, Morgan 1956; Niiler 1966) in which an inertial/frictional boundary layer is postulated to allow the flow to return to the interior. In our time-dependent model, frictional dissipation of vorticity has been replaced by an internal redistribution by eddies.

The importance of the $J(\overline{\psi', q'})$ in the maintenance of the mean gyres can be seen from Fig. 5, where $\bar{\psi}$ has been superimposed on the $J(\overline{\psi', q'})$ pattern. Regions are shaded (hatched for convergence, dotted for divergence) if $|J(\overline{\psi', q'})|$ exceeds unity, the maximum value of the wind-stress curl. Regions of significant eddy forcing are

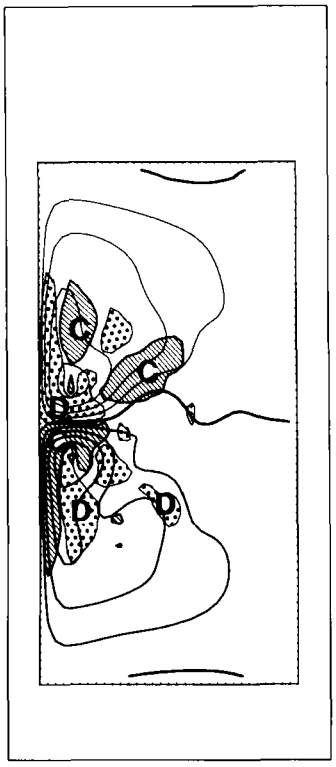

Figure 5. The $\bar{\psi}$ of Fig. 4 (C.I. = 0·3) with the eddy flux divergence pattern $J(\overline{\psi', q'})$ superimposed. Regions have been hatched for convergence and dotted for divergence, if $|J(\overline{\psi', q'})| > 1$, the maximum value of the wind-stress curl.

confined to the vicinity of the meandering jet. The $\bar{\psi}$ contours must pass through these large divergence/convergence regions before they can return to the interior. The eastward flowing jet is 'split' by the divergence/convergence, north/south dipole, as it flows into the interior after leaving the coast. There are tight recirculations on either flank, again driven by eddies.

(ii) *Eddy fluxes and the eddy enstrophy equation.* The eddy q flux, $\overline{\mathbf{v}'q'}$ is of interest because its divergence drives mean flow and also because it is the subject of parametrization schemes (see, for example, Marshall 1981). The $\overline{\mathbf{v}'q'}$ is plotted against $\bar{q}$ in Fig. 6(a). The sense of the flux is not obviously constrained by the $\bar{q}$ geometry. There are regions where it is directed up, down, and along the $\bar{q}$ gradient. In Fig. 6(b) the flux is

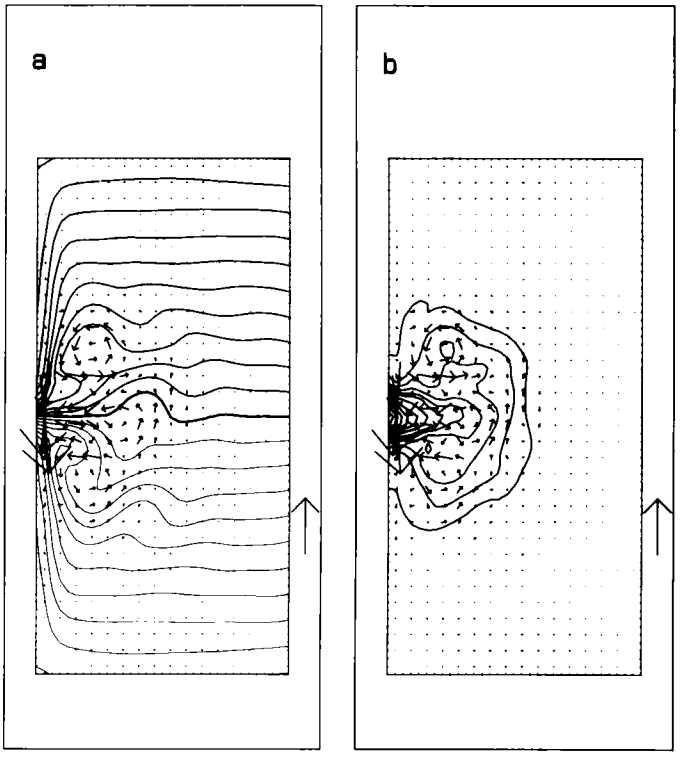

Figure 6. The eddy q flux $\overline{\mathbf{v}'q'}$ plotted against (a): $\bar{q}$ (C.I. = 0·1); (b): $\overline{q'^2}$ (C.I. = 0·05). The arrow in the margin is four units long.

plotted against the $\overline{q'^2}$ contours, and shows the presence of a contribution swirling around the $\overline{q'^2}$ contours. Figure 6 strongly suggests that the rationalization of the eddy flux provided by Eqs. (8) into contributions associated with advection and conversion of eddy enstrophy, may be helpful.

The separation of the flux depends on there being a functional relationship between $\bar{\psi}$ and $\bar{q}$, yet in the region of interest this relation is broken by large eddy flux divergences. However, in the sense that

$$\frac{|(\partial\bar{\psi}/\partial x)(\partial\bar{q}/\partial y) + (\partial\bar{\psi}/\partial y)(\partial\bar{q}/\partial x)|}{|J(\bar{\psi},\bar{q})|} \gg 1$$

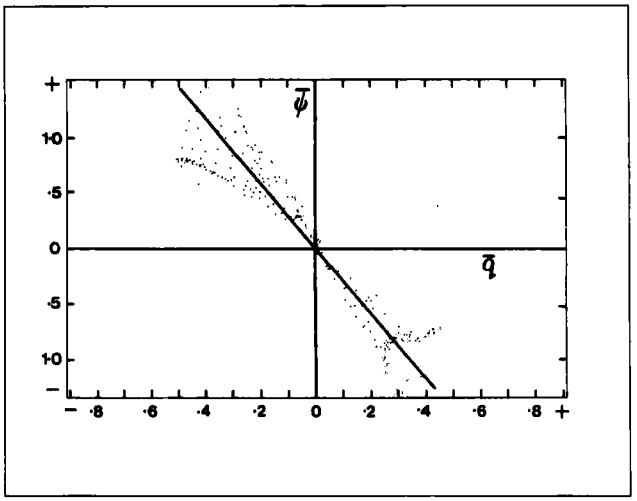

Figure 7. Scatter diagram of $\bar{\psi}$ against $\bar{q}$ in the inertial recirculation region ($0 < x < \frac{1}{2}$, $-\frac{1}{2} < y < \frac{1}{2}$) showing their functional relationship.

there remains a sufficiently close functional relationship for a separation to be helpful. The degree of scatter on the plot of $\bar{\psi}$ against $\bar{q}$, Fig. 7, attests to the existence of a relationship in the unstable jet region. The mean flow is so strong that even large eddy forcing causes only a 'small' deflection of $\bar{\psi}$ across $\bar{q}$. Figure 4(c) also indicates that the $\bar{q}$ still retains a strong constraint on the $\bar{\psi}$.

The rotational, non-divergent flux, $(\overline{\mathbf{v}'q'})_{\text{rot}}$, Eq. (8), with the $d\bar{\psi}/d\bar{q}$ approximated by the straight line in Fig. 7, is plotted in Fig. 8(a). It is mainly directed up the $\bar{q}$ gradient, responding to flow advection of $\overline{q'^2}$ from its generation region near the separation point into the interior, $\bar{\mathbf{v}} \cdot \nabla \frac{1}{2}\overline{q'^2} < 0$. Comparison with Fig. 6 shows that the $(\overline{\mathbf{v}'q'})_{\text{rot}}$ accounts for some of the major features of the spatial pattern of total flux. In particular, the along-gradient flux in the regions of $\bar{q}$ gradient reversal, and the interior up-gradient fluxes are due to the $(\overline{\mathbf{v}'q'})_{\text{rot}}$ contribution.

The remaining $\overline{\mathbf{v}'q'} - (\overline{\mathbf{v}'q'})_{\text{rot}}$ contribution is plotted in Fig. 8(b). Much of the swirl of Fig. 6 has been removed and, to a remarkable degree, this 'conversion' flux is directed not only down the gradient, but parallel to $-\nabla\bar{q}$. The divergence of this down-gradient flux gives the eddy forcing pattern of Fig. 5. So, as suggested by Marshall and Shutts (1981), the eddy flux can be illuminatingly considered to be comprised of two contributions: a rotational non-divergent 'advection' flux responding to flow advection of $\overline{q'^2}$, Eq. (8a); and a divergent 'conversion' flux responding to, and directed down the $\bar{q}$ gradient because of the dissipation of $\overline{q'^2}$ in the enstrophy cascade, Eq. (8b). In our model it is the biharmonic term which is the enstrophy-destroying friction and it makes an O(1) contribution in the eddy enstrophy budget, Eq. (6) with $\overline{D'q'} = \overline{q'\nabla^4 q'}$.

Eddy enstrophy is destroyed most vigorously in the region of *irreversible* deformation of the q contours in the unstable internal jet—see Fig. 3. The large-scale gyres advect their q contours through the boundary currents, concentrating them in the jet and creating regions of q gradient reversal. The flow becomes unstable and the contours are extended, becoming more and more convoluted, with finer and finer structure. This is the visible evidence of the cascade of q to smaller scales discussed by, for example,

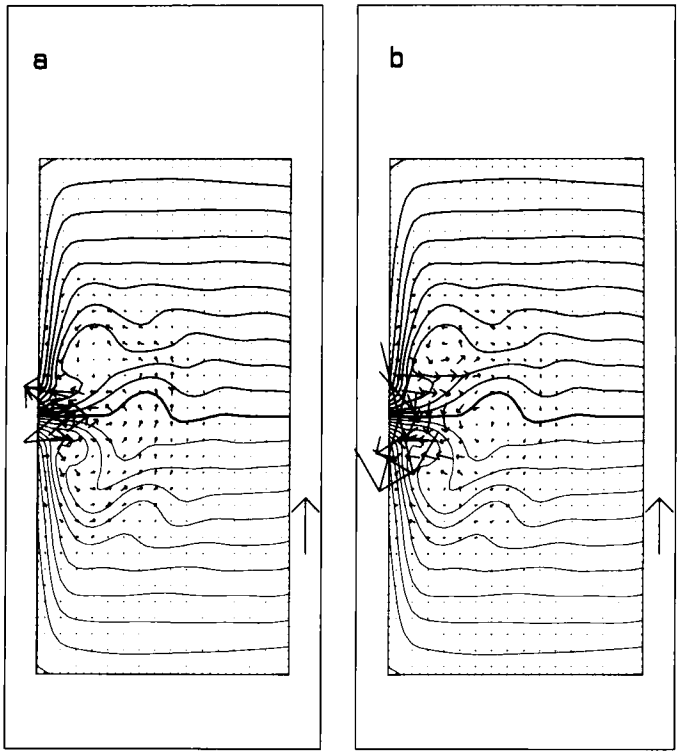

Figure 8. The separation of $\overline{\mathbf{v}'q'}$ into contributions responding to (a): advection of $\overline{q'^2}$, $(\overline{\mathbf{v}'q'})_{\text{rot}}$, Eq. (8a). This flux is non-divergent and points predominantly up-gradient, balancing the advection of $\overline{q'^2}$ from the jet into the interior. (b): dissipation of $\overline{q'^2}$ by the enstrophy cascade, $\overline{\mathbf{v}'q'} - (\overline{\mathbf{v}'q'})_{\text{rot}}$, Eq. (8b). This flux is divergent and directed down the $\bar{q}$ gradient to offset the dissipation of $\overline{q'^2}$. The fluxes are plotted against $\bar{q}$ (C.I. = 0·1) and are scaled as in Fig. 6.

Bretherton and Haidvogel (1976) and Rhines (1979). The biharmonic friction then acts at the smallest resolvable scales to dissipate the q. It is in this cascading region that the eddy conversion fluxes are large, Eq. (8b), pointing systematically down the gradient and driving mean flow.

The interiors to the north and south of the internal jet are regions where the q contours are *reversibly* deformed by the westward-propagating Rossby basin modes. There is negligible cascade, no significant eddy–mean-flow interaction and, in the time mean, a linear Sverdrup balance.

Our description of the geography of eddy fluxes and their interpretation is particularly relevant to the eddy q fluxes in the uppermost layers of quasi-geostrophic ocean models (for example, Holland and Rhines 1980). There is also some dynamical resemblance with the atmospheric storm-track event, where one often observes down-gradient fluxes at the beginning, but up-gradient fluxes at the end of the track—see Illari and Marshall (1983). As Eq. (8) makes clear, though, it should not necessarily be concluded that up-gradient fluxes are signatures of a reverse enstrophy cascade, with unravelling q contours, parcels falling back to their reference latitudes and sharpening $\bar{q}$ gradients.

Here we have concentrated on the systematic driving of mean flow by eddies: transient effects have been averaged out. In transient problems ($\partial/\partial t \neq 0$ in Eq. (6))

up-gradient fluxes can be expected wherever wave amplitudes are decaying. However, persistent changes in $\bar{q}$ are much more likely to be associated with irreversible deformation of the q contours and thus enstrophy sinks.

In conclusion of this section on eddy fluxes, it is worth emphasizing that our separation of the eddy flux into dynamically distinct contributions is not the usual separation of Lau and Wallace (1979). Lau and Wallace defined

$$\overline{\mathbf{v}'q'} = \mathbf{k}\wedge\nabla\chi + \nabla\Psi \tag{10}$$

where χ and Ψ are the streamfunction and potential for, respectively, non-divergent rotational, and divergent irrotational contributions. Taking, in turn, $\mathbf{k}\,.\,\nabla\wedge$ and $\nabla\,.$ of (10) gives

$$\left.\begin{aligned}\nabla^2\chi &= \mathbf{k}\,.\,\nabla\wedge(\overline{\mathbf{v}'q'})\\ \nabla^2\Psi &= \nabla\,.\,(\overline{\mathbf{v}'q'}).\end{aligned}\right\} \tag{11}$$

On the sphere, one solves Eqs. (11) for χ and Ψ and then computes Eq. (10), but in the closed domain of an ocean basin a unique separation is not possible, because unknown lateral boundary conditions on χ and Ψ are required to solve Eqs. (11). More important than these technical details, Eqs. (8) go beyond the purely mathematical device of Eq. (10) and separate on dynamical grounds, only identifying that non-divergent flux associated with flow advection of eddy enstrophy.

(iii) *Lateral vorticity transfer between gyres.* The central role of eddies in the equilibrium of the time-mean gyres can be appreciated by integrating Eq. (5) over the area bounded by the $\bar{\psi} = 0$ contour of the subtropical gyre. Of the 0·648 units of anticyclonic wind-stress forcing over the subtropical gyre, 0·563 is balanced by eddy vorticity flux divergence, 0·016 by bottom friction, 0·034 by biharmonic friction, and 0·029 by mean flow advection. The mean flow advection does not integrate to zero because the integrals are carried out on a grid and the $\bar{\psi} = 0$ contour, partitioning the gyres, passes between grid points: the 0·029 could be taken as the error in the discrete evaluation of the integral.

The eddies, then, transfer as much anticyclonic vorticity out of the subtropical gyre as the wind-stress curl puts in: the integral balance Eq. (9) of the single gyre has been replaced by

$$\underset{\substack{\text{along partition}\\ \text{between gyres}}}{\int \overline{v'q'}\,dx} = \int \overline{F}\,dx\,dy = \underset{\substack{\text{around periphery of}\\ \text{gyre, } \bar{\psi}=0}}{\oint \bar{\tau}\,.\,d\mathbf{l}} \tag{12}$$

expressing the line-integral of the wind-stress forcing around the periphery of the gyre. This must be balanced either by bottom friction or by 'rubbing' against the neighbouring gyre through lateral Reynold stresses. If, as here, the bottom friction is small enough, the gyres transfer vorticity via barotropic instability.

Unlike the single steady gyre, the unstable double gyres reach a (statistically) steady state in which there are extensive Sverdrup interiors (see Fig. 4), without recourse to lateral frictional boundary layers. The $\bar{\psi}_{\max}$ of the double gyre is only 1·5, thus showing that the 'singular perturbation' involved in the neglect of frictional boundary layers in the single gyre does not occur in the double gyre because of the flow instability. The internal jet must become unstable in order to achieve a balance between the cyclonic forcing over the subpolar gyre, and anticyclonic forcing over the subtropical gyre. In this way the vorticity is redistributed by the instability to offset the imbalance in the imposed forcing. It is interesting to contrast global versus local aspects of the equilibrium mech-

anism: local instability dynamics achieves the global flux of relative vorticity between the gyres. A mixed instability of a baroclinic free jet may behave differently, for with baroclinicity the relative vorticity flux can be both up and down the mean absolute vorticity gradient.

4. A PARAMETRIC REPRESENTATION OF THE GEOSTROPHIC EDDY FIELD

In section 3 the convergence/divergence pattern due to physically resolved eddies was computed and shown to bear a close relation to the $\bar{q}$ geometry: the divergence of the down-gradient eddy flux, Fig. 8(b), gives the pattern of eddy forcing, Fig. 5. Hence, even in this strong, curved flow in which $\bar{\mathbf{v}} \cdot \nabla$ cannot be neglected and where the $\bar{q}$ contours run significantly north–south, the driving of time-mean flow by eddies can be understood in terms of the divergence of a contribution to the eddy q flux directed down the local time-mean $\bar{q}$ gradient. In other words, a 'parametrization' of the local time-mean divergent eddy q flux of the form

$$(\overline{\mathbf{v}'q'})_{div} = -K\nabla\bar{q}, \tag{13}$$

where K is a positive scalar (but a function of space), still retains some validity.

As a practical demonstration of the applicability of the closure (13), the following prognostic equations for the time mean $\bar{q}$ has been integrated in place of Eq. (1):

$$R^{-1}\partial\bar{q}/\partial t + J(\bar{\psi}, \bar{q}) = \bar{F} - \bar{D} + \nabla \cdot (K\nabla\bar{q}). \tag{14}$$

The $\nabla \cdot (K\nabla\bar{q})$ serves two purposes. Firstly, it prevents the flow from becoming dynamically unstable and, secondly, it parametrizes the important transfer properties of the eddy field. The boundary conditions (2) ensure that the term integrates to zero over the basin and thus cannot generate net vorticity.

To complete the closure the magnitude and spatial variation of $K(x, y)$ need to be specified. The form of the K should reflect the horizontal scale over which the cascade (and hence the parametrization) is active. The region of irreversible deformation appears to be $R^{1/3}$ (the scale on which $\partial q/\partial y \simeq 0$). The inclusion of such scales may be of help heuristically in choosing the form of the K. However, integration of Eq. (14) has shown that the details are not important so long as the scale over which K varies is less than the $\bar{q}$ length scale. What is important is that the K should be large near the jet separation point where the enstrophy cascade enables parcels to disperse, and small in interior regions where there is no cascade, with fluid parcels remaining tied to their reference latitude. The $\overline{q'^2}$ of Fig. 6(b) has the appropriate form and is chosen here for illustrative purposes:

$$K \propto \overline{q'^2}. \tag{15}$$

The constant of proportionality is adjusted to give realistic intensity of eddy forcing.

Equation (14), with the K given by Eq. (15) and boundary conditions (2), is integrated from a state of rest in the double gyre geometry. Biharmonic and bottom frictions are retained and the non-dimensional parameters are those of section 3. Figure 9 shows the steady state solution. A close similarity with the $\bar{\psi}$ and $\bar{q}$ geometry computed from the eddy-resolving model, Fig. 4, is evident. Perhaps even more impressively, because it is a differentiated quantity, the spatial pattern of eddy flux convergence and divergence is also well reproduced parametrically: compare Fig. 9(c) with Fig. 5. Detailed comparison is not important here (if the K was computed from the eddy-resolving model using Eq. (13) as a definition, the $\bar{\psi}$ and $\bar{q}$ could be reproduced exactly) but rather the reasoning that lies behind the closure, Eq. (13). It is the association of the flow advection

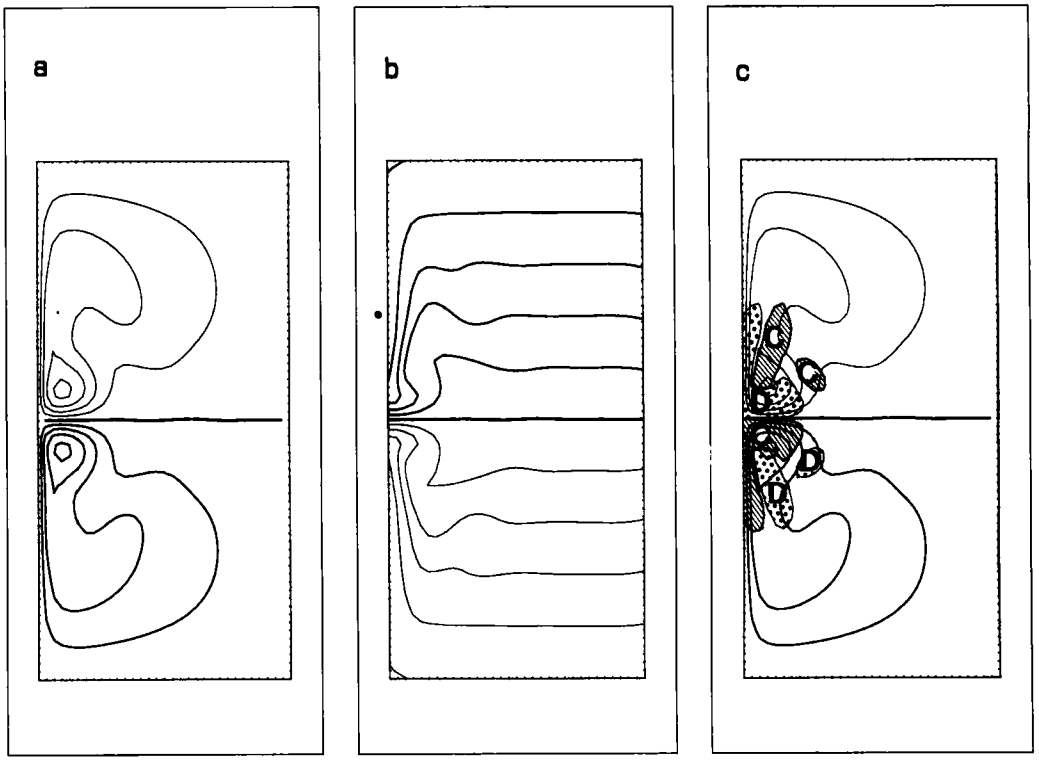

Figure 9. The steady state solution of Eq. (14) incorporating a parametric representation of the eddy field, Eq. (13). (a): $\bar{\psi}$ (C.I. = 0·3); (b): $\bar{q}$ (C.I. = 0·2); (c): $\bar{\psi}$ with the term $J(\overline{\psi', q'})$ superimposed. Regions have been hatched for convergence and dotted for divergence, as in Fig. 5.

term in the eddy variance equation with rotational *non-divergent* fluxes, demonstrated by the success of the separation, Eqs. (8), which lends strong support to a local application of a down-gradient flux parametrization for the quasi-conserved q.

Finally, we end this section with two comments on the closure. Firstly, although formally identical to that of Munk (1950) (if K is held constant) it has a completely different physical interpretation. Here it represents the redistribution of vorticity in the horizontal by a geostrophic eddy field, whereas classically it represents the transfer of momentum between the fluid and the coast in some ill-defined process confined to a lateral frictional boundary layer. Secondly, a closure for the eddy flux of the form Eq. (13) erodes the $\bar{q}$ gradients which, in the absence of external forcing to restore them, leads to an end-state in which $\bar{q}$ is uniform. In fact, this conclusion can be reached independently of any closure hypothesis by integrating Eq. (6) over a closed mean streamline and invoking the cascade (see Rhines and Young 1982).

5. Concluding remarks

The understanding of those processes which enable the ocean to circulate in gyres, despite the tendency of q contours to be latitude circles beginning and ending at the coasts, is the central objective of large-scale ocean circulation theory. Any satisfactory

explanation must recognize that the ocean is a turbulent fluid full of geostrophic eddies which have important transfer properties.

Rhines and Young (1982) describe how geostrophic eddies may erode the interior planetary vorticity gradient. At depths sufficiently remote from surface forcing, the expulsion of the $\bar{q}$ contours to the north and south by the eddy field can create extensive regions of almost uniform $\bar{q}$, allowing north–south motion and circulating gyres. In the present homogeneous model, there is a 'competition' between the advection of $\bar{q}$ contours by the gyres concentrating them into the internal jet, and the tendency of the eddy field to destroy $\bar{q}$ gradients pushing the $\bar{q}$ contours apart. Extensive plateau regions are not present because the layer is forced. The wind-stress drives flow across the $\bar{q}$ contours in the linear interior, but eddy flux divergences rather than dissipation allow the $\bar{\psi}$ to cross the $\bar{q}$ near the jet separation and in the inertial recirculation. In Lagrangian terms, parcels of water circulate through the western boundary current only exchanging planetary vorticity for relative vorticity, whilst conserving their q. Entering the unstable jet, they are taken on a meandering path allowing time for exposure to regions of opposite sign wind-stress curl forcing, and time for weak dissipation to act. Parcels recirculate, perhaps passing through the western boundary current several times before enough relative vorticity has been eroded enabling a return to the linear Sverdrup interior. Thus even the most simple barotropic ocean model is capable of providing a physically consistent picture of a possible circulation in which, relieved of frictional boundary layers, eddies can play a central and plausible role in the gyre-scale dynamics.

Recent observational studies point to the usefulness of q as a diagnostic tool in the study of the large-scale dynamics of the atmosphere and ocean. McDowell *et al.* (1982) map the potential vorticity of the North Atlantic and discuss the implications of the $\bar{q}$ geometry for the dynamics providing paths along which flow can freely move. Extensive regions of uniform potential vorticity are evident allowing the circulation to overcome the constraints of the planetary vorticity gradient. It appears, Illari and Marshall (1983), Illari (1984), that the split jet in tropospheric blocking episodes is a strong deformation field on synoptic eddies driving a cascade of q to small scales and making the block a region of almost uniform $\bar{q}$. McIntyre and Palmer (1983) describe a potential vorticity mixing event in the region of the main stratospheric vortex eroding the potential vorticity gradient.

In addition to the foregoing examples, our idealized model gyres provide a particularly simple further illustration of the different effects of wavelike and turbulent behaviour on the $\bar{q}$ distribution. The conceptual simplification provided by the focus on q and its close conservation, aids the understanding of the effect of the eddies on time-mean flow, even in the presence of the strong, curved flow of an ocean gyre. The separation of the eddy q flux into non-divergent 'advection' and divergent 'conversion' contributions, Eqs. (8), using the eddy enstrophy equation as a dynamical reference, makes transparent the sense of the local eddy q flux and its systematic effect on time-mean flow. Our analysis supports the local application of a down-gradient representation of the eddy q flux, because it has been demonstrated that the extra advection term in the time-mean eddy enstrophy equation, which vanishes in the zonal mean, is associated with non-divergent fluxes incapable of driving mean flow.

Acknowledgments

I would like to thank Drs J. S. A. Green, G. J. Shutts, M. E. McIntyre and P. B. Rhines for their comments. I am also grateful to D. R. Moore for making available his extremely rapid elliptic equation solver. This work was supported by NERC.

References

Arakawa, A. 1966 Computational design for long-term numerical integration of the equations of fluid motion: two-dimensional incompressible flow. Part 1. *J. Comput. Phys.*, **1**, 119–143

Blandford, R. R. 1971 Boundary conditions in homogeneous ocean models. *Deep-Sea Research*, **18**, 739–751

Bretherton, F. P. and Haidvogel, D. B. 1976 Two-dimensional turbulence above topography; Part 1. *J. Fluid. Mech.*, **78**, 129–154

Bryan, K. 1963 A numerical investigation of a nonlinear model of a wind-driven ocean. *J. Atmos. Sci.*, **20**, 594–606

Charney, J. G. 1955 The Gulf Stream as an inertial boundary layer. *Proc. Nat. Acad. of Sc. of U.S.A.*, **41**, 731–740

Eady, E. T. 1953 The maintenance of mean zonal surface currents, *Proceedings of Toronto Met. Conf.*, 124–128

Fofonoff, N. P. 1954 Steady flow in a frictionless homogeneous ocean. *J. Marine Res.*, **13**, 254–262

Green, J. S. A. 1970 Transfer properties of the large-scale eddies and the general circulation of the atmosphere. *Quart. J. R. Met. Soc.*, **96**, 157–185

Harrison, D. E. 1981 Eddy lateral vorticity transport and the equilibrium of the North Atlantic subtropical gyre. *J. Phys. Oceanogr.*, **11**, 1154–1158

Holland, W. R. 1978 The role of mesoscale eddies in the general circulation of the ocean–numerical experiments using a wind-driven quasi-geostrophic model. *ibid.*, **8**, 363–392

Holland, W. R. and Rhines P. B. 1980 An example of eddy induced ocean circulation. *ibid.*, **10**, 1010–1031

Illari, L. 1984 A diagnostic study of the potential vorticity in a blocking anticyclone. *J. Atmos. Sci.* (accepted)

Illari, L. and Marshall, J. C. 1983 On the interpretation of eddy fluxes in a blocking episode. *J. Atmos. Sci.*, **40**, 2232–2242

Jeffreys, H. 1926 On the dynamics of geostrophic winds. *Quart. J. R. Met. Soc.*, **52**, 85–104

Lau, N.-C. and Wallace, J. M. 1979 On the distribution of horizontal transports by transient eddies in the Northern Hemisphere wintertime circulation. *J. Atmos. Sci.*, **36**, 1844–1861

McDowell, S. Rhines, P. B. and Keffer, T. 1982 North Atlantic potential vorticity and its relation to the general circulation. *J. Phys. Oceanogr.*, **12**, 1417–1436

McIntyre, M. E. and Palmer, T. N. 1983 Breaking planetary waves in the stratosphere. *Nature*, **305**, 593–600

Marshall, J. C. 1981 On the parametrization of geostrophic eddies in the ocean. *J. Phys. Oceanogr.*, **11**, 257–271

1982 The vorticity equilibrium of ocean gyres and vorticity boundary conditions. *Ocean Modelling*, **47**, 1–3

Marshall, J. C. and Shutts, G. J. 1981 A note on rotational and divergent eddy fluxes. *J. Phys. Oceanogr.*, **11**, 1677–1680

Morgan, G. W. 1956 On the wind-driven ocean circulation. *Tellus*, **8**, 301–320

Munk, W. H. 1950 On the wind-driven ocean circulation. *J. Met.*, **1**, 79–93

Niiler, P. P. 1966 On the theory of wind-driven ocean circulation. *Deep Sea Res.*, **13**, 597–606

Pedlosky, J. 1979 *Geophysical Fluid Dynamics.* Springer-Verlag

Rhines, P. B. 1979 Geostrophic turbulence. *Ann. Rev. Fluid Mech.*, **11**, 401–441

Rhines, P. B. and Young, W. R. 1982 Homogenization of potential vorticity in planetary gyres. *J. Fluid Mech.*, **122**, 347–367

Shutts, G. J. 1983 The propagation of eddies in diffluent jetstreams: eddy vorticity forcing of 'blocking' flow fields. *Quart. J. R. Met. Soc.*, **109**, 737–761

Sverdrup, H. U. 1947 Wind-driven currents in a baroclinic ocean; with application to the equatorial currents of the Eastern Pacific. *Proc. Nat. Acad. Sci. Wash.*, **33**, 318–326

Veronis, G. 1966 Wind-driven ocean circulation. Part II: Numerical solutions of the non-linear problem. *Deep-Sea Res.*, **13**, 31–55

Welander, P. 1959 'On the vertically integrated mass transport in the oceans'. pp. 75–101 in *The Atmosphere and the Sea in Motion.* Ed. B. Bolin, Rockefeller Institute Press